Physica A 388 (2009) 1279–1288

Contents lists available at ScienceDirect

Physica A

journal homepage: www.elsevier.com/locate/physa

Recognition ability of the fully connected Hopfield neural network under a persistent stimulus field

V.M. Vieira, M.L. Lyra *, C.R. da Silva

Instituto de Física, Universidade Federal de Alagoas, 57072-970 Maceió, AL, Brazil

ARTICLE INFO

Article history:
Received 4 November 2008
Received in revised form 3 December 2008
Available online 16 December 2008

Keywords:
Neural network
Hopfield model
Biased training
Phase-diagram

ABSTRACT

We investigate the pattern recognition ability of the fully connected Hopfield model of a neural network under the influence of a persistent stimulus field. The model considers a biased training with a stronger contribution to the synaptic connections coming from a particular stimulated pattern. Within a mean-field approach, we computed the recognition order parameter and the full phase diagram as a function of the stimulus field strength h, the network charge α and a thermal-like noise T. The stimulus field improves the network capacity in recognizing the stimulated pattern while weakening the first-order character of the transition to the non-recognition phase. We further present simulation results for the zero temperature case. A finite-size scaling analysis provides estimates of the transition point which are very close to the mean-field prediction.

1. Introduction

Complex networks have been widely investigated, with a considerable growth over the last decade. The general concepts associated with their topological and dynamical behavior encounter many applications in several branches of basic and applied sciences, such as mathematics, physics, biology, engineering, computing and sociology, among others [1]. The motivations are quite broad, as for example, the use of complex network ideas to understand the dynamical aspects of multi-agent systems, such as social structures [2–5], trading markets [6,7], immunological systems [8–11] and traffic flows [12–14]. One of the most intriguing systems is neural networks, on which the correlations among their basic constituents give rise to quite complex collective behaviors which are associated with the high level capability of pattern recognition, generalization and memory [15–18].

The theoretical studies of neural networks had a great impulse during the last decades. Several models have been proposed aiming to simulate the properties of intelligent systems and the superior functions of the cerebra. The Hopfield model [19] is nowadays widely used as the prototype model of addressable memory. It essentially consists of a simple neural network of two-state basic elements connected by symmetric synapses. Besides its simplicity and preserving very few characteristics of real neural networks, the Hopfield model is able to exhibit very interesting behaviors that have a very close analogy to the memory function of biological systems.

Since the basic properties and abilities of the Hopfield model achieved a reasonable understanding, several new biologically motivated characteristics were incorporated in its dynamics such as the effects of noise [20–22], scale-free geometries [23], dilution and asymmetry [24–26], refractory periods [27–29] and external stimulus [30–41]. Usually, these features not just preserve the ability of pattern storage and recognition. In several cases, they are able to improve these functions as, for example, when considering diluted and asymmetric synapses, low pattern activity and external stimulus.

* Corresponding author.
E-mail address: marcelo@if.ufal.br (M.L. Lyra).

0378-4371/$ – see front matter © 2009 Elsevier B.V. All rights reserved.
doi:10.1016/j.physa.2008.12.025

Biologically, there are several channels that connect the nervous system with stimulus coming from the external environment such as smells, images and sounds. These signs are perceived by the sensory system and sent to the cerebra in the form of neural impulses that activate a given set of neurons. These neurons stimulate or inhibit each other thus forming a pattern in the neural network. A strong stimulus strengthens the synapses among these neurons, thus enhancing the efficiency of the network in response to such stimulus. In this sense, several proposals to incorporate the effect of an external stimulus in neural networks have been studied using both analytical and numerical techniques [31,33–37,39,40]. These models usually consider a static field conjugated to one or several patterns as well as external fields coupled to the initial network configuration.

In a previous work [41], we studied the diluted Hopfield model in the presence of a persistent stimulus. We were mainly interested in studying how the presence of a persistent stimulus on a given pattern would affect the recognition and storage capacity of the network. The parameter that controls the intensity of the persistent stimulus plays a role similar to that of an external field in magnetic systems, although it is not able to promote a symmetry breaking. We provided an exact analytical solution for the proposed model and demonstrated that the persistent stimulus can considerably increase the storage capacity when the stimulated pattern is correlated to the initial state of the network. On the other hand, when the stimulated pattern is orthogonal to the initialization pattern, recognition ability of the network is compromised.

In this work, we will analyze the effect of a persistent stimulus in the fully connected Hopfield model [19]. In a fully connected network, the Hopfield model exhibits new features that cannot be anticipated from its behavior in an ultra-diluted geometry. The analytical treatment that provides the exact solution for the dynamics of the ultra-diluted network does not apply in the fully connected regime. New approaches have to be employed to obtain approximate solutions regarding the network recognition ability. These approaches usually explore a close analogy with the thermodynamic behavior of magnetic systems with quenched disorder. In the absence of noise and stimulus, this model presents a first-order transition between a recognition phase and a non-recognition spin-glass-like phase as the number of stored patterns increases. This is in contrast with the continuous transition to the non-recognition paramagnetic-like phase observed in the ultra-diluted regime [24]. Further, in the presence of thermal noise, the fully connected network depicts a tricritical point and a reentrant phase transition not seen in the ultra-diluted regime. We will present a mean-field-like solution for the order parameters as a function of noise and stimulus field. We will report the full phase diagram of the model and show that the stimulus enhances the recognition ability and reduces the order parameter discontinuity. Further, we will present numerical simulations to show that the mean-field results reproduce quite accurately the equilibrium properties of the present neural network model.

2. The Hopfield model: Mean-field solution

A very important neural network model was introduced by Hopfield in 1982 [19]. The model exploits a close analogy of the neural network dynamics and the dynamics of disordered magnetic systems previously proposed by Little [42]. Hopfield associated the process of memorization to the problem of energy minimization in a rough energy landscape, a scenario typically found in spin-glasses.

In the Hopfield model, each neuron is seen as an Ising spin with two states. The spin state determines the nature of the electrochemical sign that it propagates to the other spins (up: excitatory signal; down: inhibitory signal). The state vector of the entire neural network is defined as:

$$\overrightarrow{S} = |S_1, S_2, \ldots, S_N\rangle. \tag{1}$$

Each neuron is connected to all other neurons of the lattice, forming a fully connected network without self-interactions. According to the Heeb rule [43], the local field acting on the ith neuron is given by:

$$J_{ij} = \frac{1}{N}\sum_{\mu=1}^{p} \xi_i^{\mu}\xi_j^{\mu}, \tag{2}$$

where ξ_i^{μ} are independent random variables assuming values ± 1 with the same probability, representing the state of ith neuron of the stored pattern μ ($\mu = 1, 2, \ldots, p$).

Based on the mean-field theory developed to treat spin-glass systems, Amit, Gutfreund and Sompolinsky [20] investigated the collective properties of the Hopfield model under the action of a thermal-like noise T. The neuron dynamics was considered to follow Little's proposal on which the time evolution of the network is governed by a stochastic dynamics rule. $S_i(t+1)$ assumes the values ± 1 with probability:

$$\Pr[S_i(t+1)] = \frac{1}{2}\left[1 + S_i(t+1)\tanh\beta h_i(t)\right], \tag{3}$$

where $\beta = 1/T$ measures the inverse of the stochastic noise level on the network, which differs from the static noise associated with the network charge, i.e., the number of stored patterns. Both sources of noise tend to make the network unstable and compromise its recognition ability. The local field h_i denotes the Hopfield post-synaptic potential,

$$h_i^{\mathrm{H}}(t) = \sum_{j=1}^{N} J_{ij}S_j(t). \tag{4}$$

Another important parameter in this model is the macroscopic overlap between the state of the system at a given time t and the stored memories, defined as

$$m_\mu(t) = \frac{1}{N}\sum_{i=1}^{N} \xi_i^\mu S_i(t). \tag{5}$$

In the long-time limit, the system achieves a statistically stationary regime on which the average order parameter m_μ can be obtained. According to the heuristic derivation developed by Geszti [44] and Peretto [45], the network recognition ability can be quantified through the following set of coupled equations:

$$\begin{aligned} m &= \int_{-\infty}^{\infty} \mathrm{D}z \tanh\left[\beta\left(m + \sqrt{\alpha r} z\right)\right], \\ r &= \frac{q}{\left[1-\beta\left(1-q\right)\right]^2}, \\ q &= \int_{-\infty}^{\infty} \mathrm{D}z \tanh^2\left[\beta\left(m + \sqrt{\alpha r} z\right)\right], \end{aligned} \tag{6}$$

where $\mathrm{D}z = \frac{\mathrm{d}z e^{-\frac{1}{2}z^2}}{\sqrt{2\pi}}$. The parameter r is known as the AGS parameter. It is associated with the squared average of the network state superposition with the other patterns stored in the network that are orthogonal to the target pattern. q is the Edward–Anderson order parameter related to a spin-glass-like state [46]. The network charge parameter $\alpha \equiv p/N$ acts as the inverse of a signal-to-noise ratio. This set of equations is equivalent to those obtained by Amit et al. [22,20,21] using the replica symmetric technique usually employed in the study of magnetic systems with quenched disorder.

In the limit of $\alpha = 0$ there is a continuous (second-order) transition from a recognition to a non-recognition phase that takes place at the critical temperature $T^* = 1$. In the absence of thermal noise, a discontinuous (first-order) transition occurs at $\alpha_c\ (T = 0) \approx 0.1379$. Amit et al. [22] were the first to provide the full phase diagram of the Hopfield model within the replica symmetric mean-field approximation, showing that $(\alpha, T) = (0, 1)$ is actually a tricritical point. They also provided numerical simulation results for the noiseless case ($T = 0$). The reported storage capacity (network charge above which the network loses its recognition ability) was found to be $\alpha_c^{\mathrm{sim}} = 0.145 \pm 0.009$, somewhat above the analytical value, an indication that there is a replica symmetry breaking close to the transition. Further analytical and numerical estimates of the transition point were latter reported [47–52] which confirmed the slight deviation from the mean-field replica symmetric result.

In the next sections, we will develop the mean-field equations for the order parameters of the fully connected Hopfield model under the influence of a stimulus field that privileges one of the patterns stored in the lattice. We will discuss the phase diagram of this model as a function of the thermal-like noise, network charge and stimulus field. Further, we will present simulation results of the noiseless case. A finite-size scaling analysis will be performed to precisely locate the transition point which will be compared with the mean-field results.

3. Persistent stimulus field in the Hopfield model

The effect of a persistent stimulus was recently introduced [41] to study the recognition capacity of the ultra-diluted Hopfield model. In such a limit, the dynamical equation giving the time evolution of the order parameter could be exactly obtained. The cases of stimulus parallel and orthogonal to the pattern correlated to the network initial state were analyzed. A practical way to introduce the stimulus field is through a local field term while keeping all the other network characteristics unchanged. The local field assumes the form

$$h_i(t) = h_i^{\mathrm{H}}(t) + h_i^{\mathrm{S}}(t), \tag{7}$$

where $h_i^{\mathrm{H}}(t)$ is the usual local field of the Hopfield model, as defined in the previous section. The additional local field $h_i^{\mathrm{S}}(t)$ represents a stimulus directed to one of the stored pattern which is written as

$$h_i^{\mathrm{S}}(t) = h m_\nu(t) \xi_i^\nu, \tag{8}$$

where ξ^ν is the stimulated pattern, $m_\nu(t)$ is the state superposition with the stimulated pattern (macroscopic overlap) at time t and h is a parameter to control the amplitude of the stimulus. Notice that such a stimulus acts only when the network state has a macroscopic superposition with the stimulated pattern.

As written above, the stimulus field acts during the network recognition dynamics. This form allows for a direct extension of the mean-field equations for the fully connected Hopfield model. The local field depends of the network macroscopic superposition with the stimulated pattern. An alternative and equivalent representation of the stimulus field can be obtained when its effect is incorporated during the network training stage. The total local field can be put in the form

$$h_i(t) = \sum_{j=1}^{N} J_{ij}^{\mathrm{eff}} S_j(t), \tag{9}$$

where J_{ij}^{eff} is the effective synaptic coupling given by

$$J_{ij}^{\text{eff}} = \frac{1}{N}\sum_{\mu\neq\nu}\xi_i^\mu\xi_j^\mu + \frac{1}{N}(1+h)\,\xi_i^\nu\xi_j^\nu. \tag{10}$$

The last term of the above equation is responsible for the strengthening of the synaptic connections during the network training which produces a bias in the recognition dynamics towards the stimulated pattern ν when $h_0 > 0$. In this sense, such a stimulus field acquires a direct biological interpretation because biased memory can be produced by an unusual experience which has a stronger influence in the formation of the neuron synapses than the regular experiences. Such a modification in Hebb's rule is known to promote the enhancement of learning either a finite [30,38] or infinite [32] number of marked patterns without losing the ability to retrieve the unmarked ones.

3.1. Mean-field equations and phase diagram

Considering the initial state of the network as the pattern ν that is under the influence of the persistent stimulus, the heuristic derivation proposed by Geszti [44] and Peretto [45] can be extended to obtain the equilibrium average order parameter.

In general, the time evolution of the neuron at site i depends on the local field $h_i(t)$. Such a local field is a function of the fluctuating variables $S_j(t)$ that represent the state of all neurons in the network. Within a mean-field prescription, where a stochastic noise $T = 1/\beta$ plays a role similar to the temperature in disordered magnets, one can write the macroscopic overlap between the network state and one of the stored patterns as

$$m_\delta(t+1) = \frac{1}{N}\sum_{i=1}^{N}\xi_i^\delta\xi_i^\nu\tanh\beta\tilde{m}, \tag{11}$$

where

$$\tilde{m} = m_\nu(t)\,(1+h) + \sum_{\mu\neq\nu}^{p} m_\mu(t)\xi_i^\mu\xi_i^\nu. \tag{12}$$

This is the most general expression for the network superposition with a given pattern δ. The first term of the last equation represents the signal ν and brings the influence of the stimulus field. The other term acts as an effective noise produced by the remaining stored patterns and generates an instability that can destroy the superposition, thus leading to a non-recognition phase.

Considering the stored patterns as uncorrelated, we can assume that $m_{\mu\neq\nu} \ll 1$. Therefore, for $\delta \neq \nu$, the expansion of the hyperbolic tangent up to second order results in

$$m_\delta(t+1) \approx \frac{1}{N}\sum_{i=1}^{N}\xi_i^\delta\xi_i^\nu\tanh\left[\beta\left(m_\nu(t)(1+h)+\zeta(t)\right)\right] + \beta m_\delta(t) - \beta q_\nu m_\delta(t), \tag{13}$$

where $\zeta(t) = \sum_{\mu\neq\nu,\delta}^{p} m_\mu(t)\xi_i^\mu\xi_i^\nu$ is a noise term associated with the network charge and we defined the quantity

$$q_\nu(t) = \frac{1}{N}\sum_{i=1}^{N}\tanh^2\left[\beta\left(m_\nu(t)(1+h)+\zeta(t)\right)\right]. \tag{14}$$

Up to this point, the above equations describe exactly the network dynamics. In order to achieve the equilibrium macroscopic superposition, we will assume that in the long-time regime these equations will converge to a fixed point solution ($m_\delta(t+1) = m_\delta(t) = m_\delta$). Further, we will consider that the noise terms appearing in these equations are independent random variables with zero mean and variance given by the sum of the variances of each term. With this reasoning, the total noise can be assumed as having a Gaussian distribution. Within these assumptions, and considering the limit of $p \to \infty$ and $N \to \infty$ while keeping $\alpha \equiv p/N$ finite, one can achieve the following self-consistent equations for the network superposition with the stimulated pattern;

$$\begin{aligned} m &= \int_{-\infty}^{\infty} \mathrm{D}z\,\tanh\left\{\beta\left[m\,(1+h)+\sqrt{\alpha r}z\right]\right\},\\ r &= \frac{q}{\left[1-\beta\,(1-q)\right]^2},\\ q &= \int_{-\infty}^{\infty} \mathrm{D}z\,\tanh^2\left\{\beta\left[m\,(1+h)+\sqrt{\alpha r}z\right]\right\}, \end{aligned} \tag{15}$$

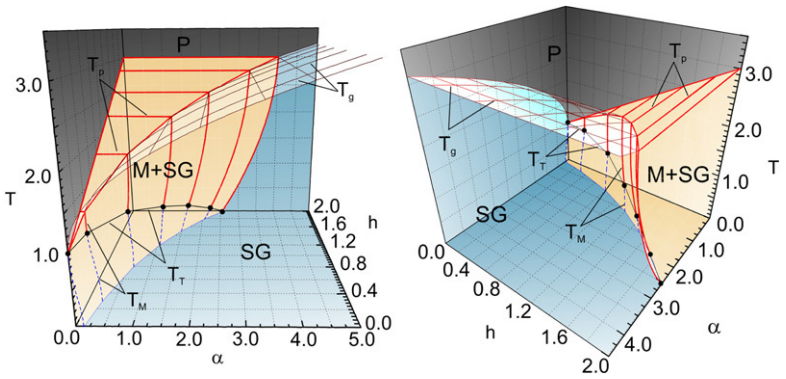

Fig. 1. (Color Online) Phase diagram in the $T \times \alpha \times h$ space. Two perspectives of the parameters space are shown for better visualization. The dashed lines represent first-order transitions while solid lines stand for continuous second-order transitions. The filled circles locate the tricritical points. The clear region (M + SG) represents the recognition phase with $m \neq 0$ while the darker region at high temperatures (P) is similar to a paramagnetic phase with $m = q = 0$. The region with intermediate tonality (blue in color) is a spin-glass-like phase (SG) with $m = 0$, $q \neq 0$.

from which we omitted the subscript ν in the order parameters. For $h = 0$, we recover the set of equations for the fully connected unbiased Hopfield model. To solve this set of equations, we employed the same methodology used by Naef and Canning [53] based on the Newton–Raphson algorithm in three variables. In Fig. 1, we present the phase diagram in the $T \times \alpha \times h$ space. In particular, we reproduce the phase diagram reported by Amit [21] in the limit of $h = 0$.

For $h > 0$, we observe a considerable increase of the recognition region. The phase diagram exhibits the same three basic phases presented by the usual Hopfield model without stimulus. One of the phases is equivalent to the paramagnetic (P) phase of magnetic systems with the trivial solution $m = q = 0$. A second phase with many stable states with no correlation with the stored patterns is similar to the spin-glass (SG) magnetic phase whose fixed point solution has $m = 0$ and $q \neq 0$. The last region is the recognition phase closely correlated to the ordered magnetic (M + SG) phase having a non-trivial solution for both m- and q-order parameters. As the stimulus field increases, this solution becomes more robust against both thermal and static noises [38].

The above three phases are separated in the phase diagram by the following curves:

- The curves $T_P(h) = 1 + h$, for $0 \leq \alpha \leq h^2$, separate the magnetic phase(**M** + **SG**) from the paramagnetic phase (**P**) through a continuous (second-order) transition.
- The curves $T_g = 1 + \sqrt{\alpha}$, with $\alpha \geq h^2$, separate the spin-glass phase **SG** from the paramagnetic phase **P**, also through a continuous (second-order) transition.
- The curves T_M, which do not have a simple analytical expression, separate the ordered magnetic phase **M** + **SG** from the spin-glass phase **SG**. This transition can be either continuous or discontinuous depending on the parameters h and α. A line of tricritical points T_T delimits these two regimes.

In the absence of stimulus ($h = 0$), the system presents a tricritical point at $(\alpha, T) = (0, 1)$. The location of the tricritical points for $h > 0$ is represented by filled circles in the phase diagram for some representative values of the stimulus field. The black solid line is the estimated curve T_T of tricritical points. It reaches $T = 0$ for $h = 2$. Above this field the transition becomes continuous at any temperature. The order of the transition was determined from the analysis of the order parameters' behavior as a function of the thermal-like noise T for distinct values of the stimulus field h and network charge α, as shown in Fig. 2.

The large static noise originated by an elevated number of stored patterns, i.e., by a large network charge α, promotes the appearance of several local energy minima which makes the network unstable and susceptible to errors in the recognition process. This fact is responsible for a decrease of the macroscopic superposition m in the vicinity of the transition from the ordered to the spin-glass phase. The thermal noise T acts distinctly on the network. It generates fluctuations that remove the network from local energy minima. These distinct trends played by the thermal and static noises result in the reentrant behavior of the transition line, which becomes more pronounced as the stimulus field is increased.

3.1.1. *Deterministic case*

For the particular case of $T = 0$, we can reduce the set of Eq. (15) to

$$\begin{aligned} m &= \operatorname{erf}\left[\frac{m\,(1+h)}{\sqrt{2\alpha r}}\right], \\ r &= \frac{1}{(1-C)^2}, \\ C &= \sqrt{\frac{2}{\pi\alpha r}}\exp\left[-\frac{m^2\,(1+h)^2}{2\alpha r}\right], \end{aligned} \tag{16}$$

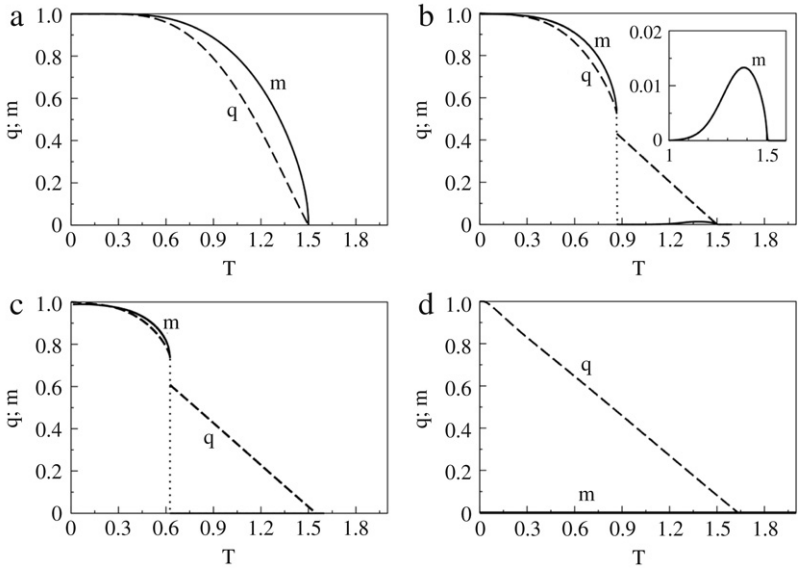

Fig. 2. Order parameters q and m versus the thermal-like noise T for the stimulus field $h = 0.5$ and (a) $\alpha = 0.05$, (b) $\alpha = 0.245$, (c) $\alpha = 0.3$ and (d) $\alpha = 0.4$. For $\alpha = 0.05$ the transition is continuous from the ordered magnetic to the paramagnetic-like phase. For $\alpha = 0.3$ there are two transitions: a discontinuous transition from the ordered to the spin-glass phase followed by a continuous transition to the paramagnetic-like phase. At $\alpha = 0.245$ one observes the revival of the ordered magnetic phase, signaling the reentrant structure of the transition line T_M. For $\alpha = 0.4$, we are in a non-recognition phase and $m = 0$. In this case there is a continuous transition from the spin-glass to the paramagnetic-like phase.

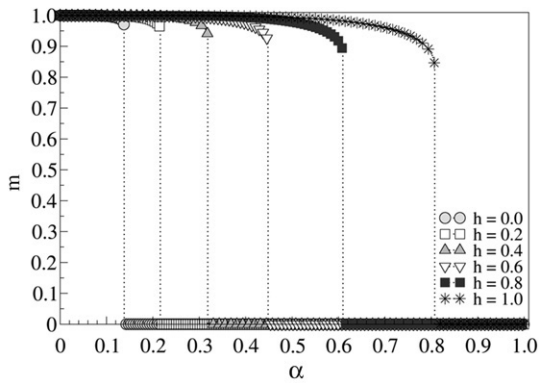

Fig. 3. Order parameter m as a function of the network charge α for $T = 0$ and distinct stimulus fields h. At $\alpha_c(h)$ the system undergoes a discontinuous transition from the recognition to the non-recognition phase. The order parameter jump decreases when the stimulus is increased, pointing to a possible continuous transition at large fields.

where $\mathrm{erf}(x) = \frac{2}{\pi}\int_0^x e^{-u^2} du$ is the usual error function and $C = \lim_{\beta\to\infty} \beta(1-q)$. The transformation $y = m\,(1+h)\,/\sqrt{2\alpha r}$ allows us to write the following transcendental equation that can be numerically solved:

$$\mathrm{erf}\,(y) = \frac{y}{1+h}\left(\sqrt{2\alpha} + \frac{2}{\sqrt{\pi}} e^{-y^2}\right). \tag{17}$$

Below a critical network storage capacity α_c, non-trivial solutions with $m \neq 0$ are obtained. The dependence of the order parameter m on the network charge α and the stimulus field h can be numerically found, as reported in Fig. 3. The main effect of the stimulus field is to enhance the network storage capacity α_c. In the vicinity of the transition, the network recognizes the stored pattern with an error fraction that is larger than that in the zero field case. The enhancing of the network storage capacity and the decreasing of the order parameter jump at the transition are reported in Fig. 4.

For $h = 0$, we recover $\alpha_c \simeq 0.138$ as obtained by Amit et al. [22] for the usual Hopfield model. Along the line $\alpha_c(h)$ (Fig. 4(a)) the transition from the recognition to the non-recognition phase is discontinuous up to $h = 2$ on which $\alpha_c = 8/\pi \simeq 2.5465$, as firstly reported in Ref. [30]. This is a tricritical point separating the regime of discontinuous and continuous transitions. This analytical value coincides with the one reported in the main phase diagram (Fig. 1) obtained through the numerical Newton–Raphson algorithm. After the tricritical point, the second-order transition takes place at $\alpha_c = 2h^2/\pi$.

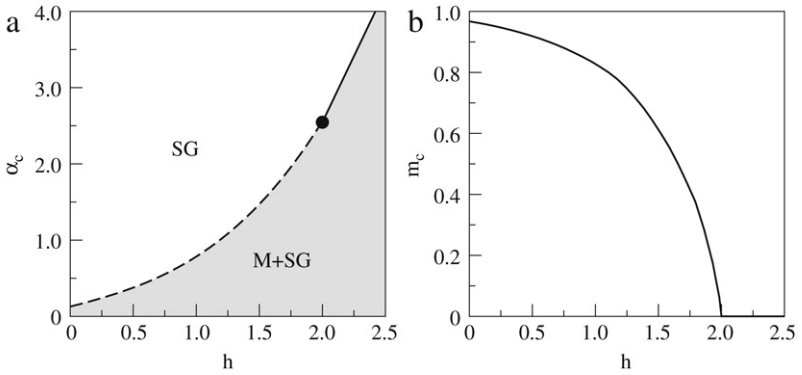

Fig. 4. (a) Network storage capacity $\alpha_c \times h$ and (b) Recognition order parameter at the transition $m_c \times h$ for $T = 0$. In (a) the region (M + SG) represents the recognition phase while the region (SG) stands for the non-recognition spin-glass-like phase. Dashed (solid) line indicates a discontinuous (continuous) transition. In (b) the order parameter jump at the transition vanishes at $h = 2$. Above this field the transition becomes continuous.

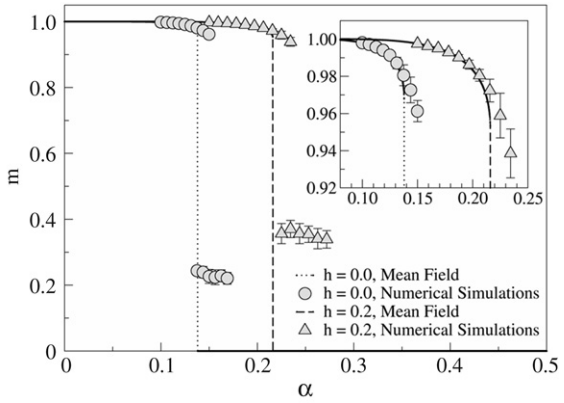

Fig. 5. Average equilibrium superposition with the initial state $m \times \alpha$ for a network with $N = 32\,000$ neurons. Both cases of no stimulus ($h = 0.0$) and weak stimulus ($h = 0.2$) were considered. The solid lines represent the mean-field prediction while the symbols give the simulation results. Averages were taken over 100 distinct samples having independent sets of stored patterns. The mean-field prediction shows a very good agreement with the simulations. The jump in the average superposition signals the discontinuous transition to the non-recognition phase. The finite superposition after the transition is a finite-size effect. The inset is an amplification of the average superposition near the transition to show that the discontinuity decreases in the presence of the stimulus field, in agreement with the mean-field prediction.

3.2. Numerical simulations at $T = 0$

In this section, we compare the mean-field results with numerical simulations performed at $T = 0$. Our simulations used a multi-spin-coding algorithm that allows a higher computational efficiency when simulating systems involving Boolean random variables [54]. Our main interest was to locate the network storage capacity for distinct values of the stimulus field. To achieve this, we followed the procedure developed by Stiefvater et al., [51] when studying the critical behavior of the usual Hopfield model. The proposed scheme explores finite-size scaling ideas.

In our simulations, the initial state of the system was taken as one of the p stored patterns. These patterns were generated at random with no correlation between them. During the network time evolution, the state of the neuron i at time t was set equal to the sign of the total local field $h_i(t)$. After a long time, the network reaches a stationary state. In this regime, we compute the average superposition between the network final and initial states. We performed averages over distinct sets of stored patterns. Such a computation was repeated for networks with different number of neurons N to allow for a proper finite-size scaling analysis.

In Fig. 5, we present the order parameter m as a function of the network charge α both in the absence of the persistent stimulus $h = 0$, as well as under the influence of a weak stimulus field $h = 0.2$. The mean-field prediction based on the set of Eq. (16) is shown together with the simulation results. In the simulations, we used a network with $N = 32\,000$ neurons and averaged the equilibrium superposition over 100 samples having distinct sets of uncorrelated stored patterns. The simulation data corroborate the discontinuous transition to the non-recognition phase. The main dependence on the stimulus field h of both the critical point location and the order parameter discontinuity is consistent with the mean-field analysis. The finite superposition after the transition is a finite-size effect and decreases slowly as the system size is increased. Such two state stability is typical of systems in the vicinity of a first-order transition and a finite-size scaling study can provide a precise estimate of the transition point in the thermodynamic limit of $N \to \infty$, as described below.

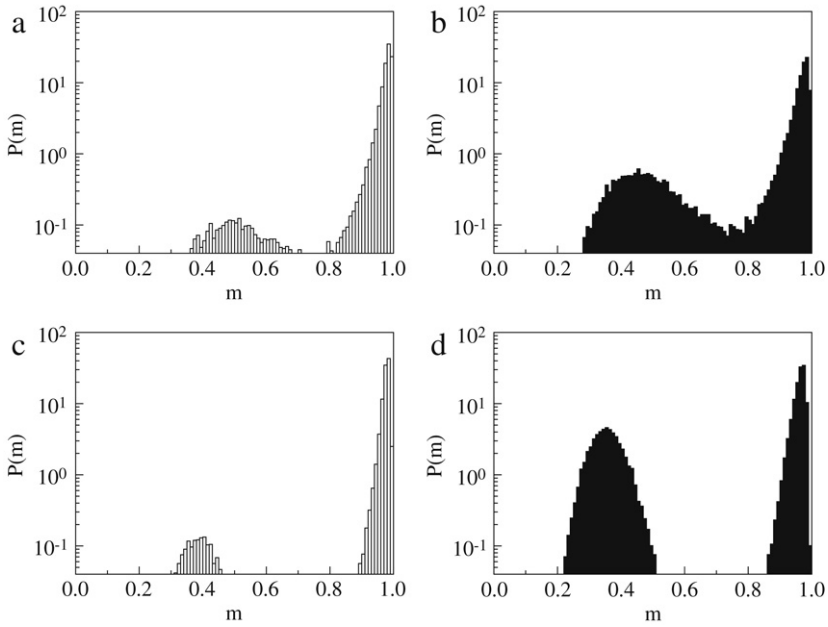

Fig. 6. Probability distribution function of the macroscopic superposition m for $h = 0.1$. Top panels: $N = 2048$ with (a) $\alpha = 0.17383$, (b) $\alpha = 0.18555$. Bottom panels: $N = 8192$ with (c) $\alpha = 0.17383$, (d) $\alpha = 0.18555$. Notice that, when the network size is increased, the fraction of samples that reach the low-recognition peak decreases below the critical point. This trend is reverted after the transition. Histograms were obtained from 60 000 distinct sets of stored patterns.

For large enough networks, the distribution function of the macroscopic superposition m develops a two peak structure near the first-order transition, as shown in Fig. 6. The position of the first peak slowly decreases as the network size increases. It corresponds to an asymptotically non-recognition state. The second peak represents recognition solutions. These peaks become broader as the stimulus field increases up to the regime of a single peak distribution signaling the set up of the second-order transition. In what follows we will analyze the finite-size scaling behavior in the regime of weak stimulus where the transition remains strongly first order.

In the recognition phase, the fraction f of samples that reach the non-recognition peak decreases with increasing system sizes. The opposite behavior is attained after the transition to the non-recognition phase. These trends are clearly depicted in Fig. 6. This specific feature can be used to give a precise estimate of the network storage capacity. In the vicinity of the first-order transition, the average fraction f of samples whose dynamics leads to a final configuration with macroscopic superposition belonging to the recognition peak scales with the network size N according to the following relation [51]:

$$\langle \ln(f) \rangle = g[(\alpha - \alpha_c)N], \tag{18}$$

where the brackets stand for an average over distinct measures of the distribution function. The scaling function g vanishes in the limit of $(\alpha - \alpha_c)N \to -\infty$, signaling that the asymptotic average fraction $f \to 1$ in the recognition phase. In the opposite limit of $(\alpha - \alpha_c)N \to +\infty$ the scaling function $g \to -\infty$ because $f \to 0$ in the non-recognition phase. At the critical point the scaling function $g(0)$ assumes a constant value, independent of the system size. Therefore, curves of $\langle \ln(f) \rangle$ computed for different network sizes shall intercept at a common point locating the network storage capacity α_c.

To employ the above scaling analysis, we simulated networks with $N = 2048$, 4096 and 8192 neurons for a range of α values close to the transition from the recognition to the non-recognition phase. For each value of α and N, we firstly used 100 initial sets of stored patterns to compute the fraction f. This procedure was repeated 200 times to perform the logarithmic average $\langle \ln(f) \rangle$. Our main results for the cases of no stimulus field and a weak stimulus field are summarized in Fig. 7. In each case, the interception of the curves exhibits a very small spread which indicates that scaling corrections are very small for the system sizes simulated. The location of the transition point in the absence of stimulus reproduces accurately previous estimates [51,52]. For the weak field $h = 0.1$, the estimated network storage capacity is very close, although slightly above our mean-field prediction. Such a small difference between the mean-field and simulation estimates of the storage capacity has already been pointed out to occur also for the usual Hopfield model. Its origin is associated with a possible replica symmetry breaking taking place at the vicinity of the transition to the spin-glass-like state.

The present finite-size scaling scheme gives very accurate estimates of the transition point. However, such a method requires the double peak structure in the order parameter distribution to be well defined with no considerable superposition. For a strong first-order transition, the splitting of the order parameter distribution function can be achieved even for relatively small networks. Therefore, the present finite-size scaling analysis can be performed with a considerably small computational effort. This is the case of weak stimulus fields. As we have shown in the previous sections, the order

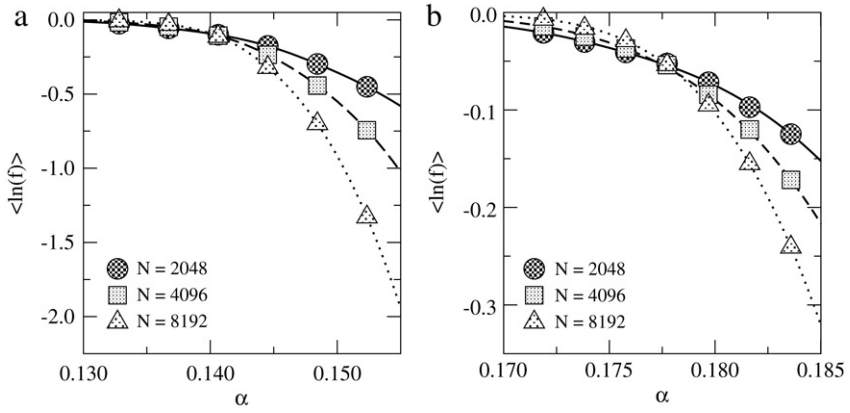

Fig. 7. $\langle \ln(f) \rangle$ as a function of $\alpha = p/N$, for network sizes $N = 2048$, 4096 and 8192 for the cases of (a) no stimulus and (b) weak stimulus. Symbols are the simulation results. The solid lines represent spline interpolations. The interception point locate the network storage capacity above which there is no recognition ability. In the absence of a stimulus field, the storage capacity $\alpha_c(h = 0) = 0.140(1)$, in agreement with previous estimates. For a weak stimulus field $h = 0.1$ the storage capacity becomes $\alpha_c(h = 0.1) = 0.178(1)$ which is very close to the mean-field prediction.

Table 1
The storage capacity α_c for distinct values of the stimulus field h as obtained from the finite-size scaling analysis of simulation data, together with the corresponding mean-field estimates. The small difference between these two values is outside the error bars which indicates that a replica symmetry breaking occurs at the vicinity of the transition to the spin-glass-like non-recognition phase.

h	α_c	α_c^{mf}
0.0	0.140 ± 0.001	0.138
0.1	0.178 ± 0.001	0.174
0.2	0.221 ± 0.001	0.216

parameter discontinuity at the transition decreases with increasing stimulus, approaching to a tricritical point above which the transition becomes second order. In the regime of weak first order, the splitting of the two peaks can only be observed for very large network sizes which compromises the efficiency of the present method. In Table 1, we compare our simulation and mean-field estimates of the network storage capacity α_c in the regime of null and weak stimulus fields.

4. Summary and conclusions

In summary, we investigated the influence of a persistent stimulus field in the recognition ability of the fully connected Hopfield model. The model considers that the stimulated pattern has a stronger influence in the training process during which the synaptic connections between the network neurons are settled. From the biological point of view, such biased training may reflect the fact that an unusual (e.g. traumatic) experience can produce stronger synaptic connections than usual daily experiences. The stimulus effectively generates an additional local field on each neuron that is proportional to the macroscopic superposition of the network state with the stimulated pattern.

We developed a replica symmetric mean-field solution for the recognition order parameter and obtained the full phase diagram as a function of the stimulus field h, a thermal-like noise T and the network charge α. The stimulus field increases the network capacity to recognize the stimulated pattern. On the other hand, it weakens the discontinuous nature of the transition to the non-recognition phase. A line of tricritical points separating the regimes of first-order and second-order transitions was obtained. The transition always becomes continuous for $h > 2$. Further, we obtained that the stimulus field enhances the reentrant character of the transition as a function of the thermal noise.

Further, we employed a finite-size scaling analysis of data obtained from simulations at zero temperature. The scaling scheme that we used explores the double peak structure of the order parameter distribution function at the vicinity of strong first-order transitions. In the weak stimulus field regime, the finite-size scaling estimate for the network storage capacity was found to be very close, although slightly above, the replica symmetric mean-field prediction. This is consistent with the previous works showing that replica symmetry breaks very close to the spin-glass-like transition to the non-recognition phase. Here the employed finite-size scaling analysis becomes computationally inefficient in the regime of weak first-order transition and inadequate to deal with continuous transitions. Alternative schemes would be required in order to evaluate the accuracy of the replica symmetric solution in these regimes.

Acknowledgements

We would like to thank the partial financial support from FINEP, CAPES and CNPq-Rede Nanobioestruturas (Brazilian Research Agencies) as well as from FAPEAL (Alagoas State Research Agency).

References

[1] S. Boccaletti, S. Latora, Y. Moreno, M. Chavez, D.U. Hwang, Phys. Rep. 424 (2006) 175.
[2] M.E.J. Newman, M. Girvan, Phys. Rev. E 69 (2004) 026113.
[3] P.G. Lind, L.R. da Silva, J.S. Andrade, H.J. Herrmann, Phys. Rev. E 76 (2007) 036117.
[4] W. Li, X. Zhang, G. Hu, Phys. Rev. E 76 (2007) 045102(R).
[5] M. Nekovee, Y. Moreno, G. BianconiG, M. Marsili, Physica A 374 (2007) 457.
[6] G. Bonanno, G. Caldarelli, F. Lillo, R.N. Mantegna, Phys. Rev. E 68 (2003) 046130.
[7] J. Jiang, W. Li, X. Cai, Physica A 387 (2008) 528.
[8] R. Cohen, S. Havlin, D. ben-Avraham, Phys. Rev. Lett. 91 (2003) 247901.
[9] M. Brede, U. Behn, Phys. Rev. E 67 (2003) 031920.
[10] L.C. Ribeiro, R. Dickman, A.T. Bernardes, N.M. Vaz, Phys. Rev. E 75 (2007) 031911.
[11] W.H. Bai, T. Zhou, B.H. Wang, Physica A 384 (2007) 656.
[12] B. Tadic, S. Thurner, G.J. Rodgers, Phys. Rev. E 69 (2004) 036102.
[13] L. Zhao, Y.C. Lai, K. Park, N. Ye, Phys. Rev. E 71 (2005) 026125.
[14] W. Han-Jun, G. Zi-You, S. Hui-Jun, Physica A 387 (2008) 1025.
[15] D.J. Amit, Modeling Brain Function: The World of Attractor Neural Networks, Cambridge University Press, Cambridge, 1989.
[16] J. Hertz, A. Krogh, R.G. Palmer, Introduction to the Theory of Neural Computation, Addison-Wesley, Santa Fe, 1991.
[17] G.L. Pellegrini, L. de Arcangelis, H.J. Herrmann, C. Perrone-Capano, Phys. Rev. E 76 (2007) 016107.
[18] J.P. Eckmann, O. Feinerman, L. Gruendlinger, E. Moses, J. Soriano, T. Tiusty, Phys. Rep. 449 (2007) 54.
[19] J.J. Hopfield, Proc. Natl. Acad. Sci. USA 79 (1982) 91.
[20] D.J. Amit, H. Gutfreund, H. Sompolinsky, Phys. Rev. A 32 (1985) 1007.
[21] D.J. Amit, H. Gutfreund, H. Sompolinsky, Phys. Rev. Lett. 55 (1985) 1530.
[22] D.J. Amit, H. Gutfreund, H. Sompolinsky, Ann. Phys. 173 (1987) 30.
[23] D. Stauffer, A. Aharony, L.D. Costa, J. Adler, Eur. Phys. J. B 32 (2003) 395.
[24] B. Derrida, E. Gardner, A. Zippelius, Europhys. Lett. 4 (1987) 167.
[25] C.R. da Silva, L. da Silva, F. Tamarit, Internat. J. Modern Phys. C 9 (1998) 31.
[26] D. Bollé, G. Jongen, Eur. Phys. J. B 16 (2000) 749.
[27] C.R. da Silva, F.A. Tamarit, E.M.F. Curado, Phys. Rev. E 55 (1997) 3320.
[28] F.A. Tamarit, D.A. Stariolo, S.A. Cannas, P. Serra, Phys. Rev. E 53 (1996) 5146.
[29] C.R. da Silva, Physica A 301 (2001) 362.
[30] J.F. Fontanari, R. Köberle, J. Phys. A: Math. Gen. 21 (1988) L253.
[31] D.J. Amit, G. Parisi, S. Nicolis, Network: Comput. Neural Syst. 1 (1990) 75.
[32] S. Nicolis, Europhys. Lett. 12 (1990) 583.
[33] H.W. Yau, D.J. Wallace, J. Phys. A: Math. Gen. 24 (1991) 5639.
[34] A. Engel, M. Bouten, A. Komoda, R. Serneels, Phys. Rev. A 42 (1990) 4998.
[35] H. Englisch, Y. Xiao, K. Yao, Phys. Rev. A 44 (1991) 1382.
[36] Y.Q. Ma, Y.M. Zhang, Y.G. Ma, C.D. Gong, Phys. Rev. E 47 (1993) 3985.
[37] Y.Q. Ma, C.D. Gong, Phys. Rev. E 51 (1995) 1573.
[38] D. Bollé, J. Huyghebaert, Phys. Rev. E 51 (1995) 732.
[39] P. Shukla, Phys. Rev. E 56 (1997) 2265.
[40] M.P. Singh, Phys. Rev. E 64 (2001) 051912.
[41] G.A. Sobral, V.M. Vieira, M.L. Lyra, C.R. da Silva, Phys. Rev. E 74 (2006) 046117.
[42] W.A. Little, Math. Biosci. 19 (1974) 101.
[43] D.O. Heeb, The Organization of Behavior: A Neuropsychological Theory, Wiley, New York, 1949.
[44] T. Geszti, Physical Models of Neural Network, World Scientific, Singapore, 1990.
[45] P. Peretto, J. Physique 49 (1988) 711.
[46] S.F. Edward, P.W. Anderson, J. Phys. F 5 (1975) 965.
[47] A. Crisanti, D.J. Amit, H. Gutfreund, Europhys. Lett. 2 (1986) 337.
[48] H. Horner, D. Bormann, M. Frick, H. Kinzelbach, A. Schmidt, Z. Phys. B 76 (1989) 381.
[49] G.A. Kohring, J. Phys. A 23 (1990) 2237.
[50] H. Steffan, R. Kühn, Z. Phys. B 95 (1994) 249.
[51] T. Stiefvater, K.R. Müller, R. Kühn, Physica A 232 (1996) 61.
[52] S. Risau-Gusman, M.A.P. Idiart, Phys. Rev. E 72 (2005) 041913.
[53] J.P. Naef, A. Canning, J. Physique 2 (1992) 247.
[54] T.J.P. Penna, P.M.C. Oliveira, J. Phys. A: Math. Gen. 22 (1989) 719.